MODELING AND CHARACTERIZATION OF GRAPHENE FOR EFFICIENT MILLIMETERWAVE AND TERAHERTZ ANTENNAS

By

MOHAMMED TAIH GATTE
(1340810872)

A thesis submitted in fulfillment of the requirements for the degree of Doctor of Philosophy

School of Computer and Communication Engineering
UNIVERSITI MALAYSIA PERLIS

2017

UNIVERSITI MALAYSIA PERLIS

DECLARATION OF THESIS

Author's full name : MOHAMMED TAIH GATTE

Date of birth : 1st July 1968

Title : Modeling and Characterization of Graphene for Efficient Milimeterwave and Terahertz Antennas

Academic Session : 2016/2017

I hereby declare that the thesis becomes the property of Universiti Malaysia Perlis (UniMAP) and to be placed at the library of UniMAP. This thesis is classified as:

☐ **CONFIDENTIAL** (Contains confidential information under the Official Secret Act 1972)

☐ **RESTRICTED** (Contains restricted information as specified by the organization where research was done)

■ **OPEN ACCESS** I agree that my thesis is to be made immediately available as hard copy or on-line open access (full text)

I, the author, give permission to the UniMAP to reproduce this thesis in whole or in part for the purpose of research or academic exchange only (except during a period of _ years, if so requested above).

Certified by:

SIGNATURE	**SIGNATURE OF SUPERVISOR**
A3698300	**Dr. Ping Jack Soh**
(NEW IC NO. / PASSPORT NO.)	**NAME OF SUPERVISOR**
Date: ______________	Date: ______________

GRADUATE SCHOOL
UNIVERSITY MALAYSIA PERLIS

PERMISSION TO USE

In presenting this thesis in fulfilment of a post graduate degree from the Universiti Malaysia Perlis, I agree that permission for copying of this thesis in any manner, in whole or in part, for scholarly purposes may be granted by my supervisor(s) or, in their absence, by the Dean of the Graduate School. It is understood that any copying or publication or use of this thesis or parts thereof for financial gain shall not allowed
without any written permission. It is also understood that due recognition shall be given to me and to Universiti Malaysia Perlis for any scholarly use which may be made of any material from my thesis

Request for permission to copy or to make other use of material in this thesis whole or in part should be addressed to

Dean of Graduate School
Universiti Malaysia Perlis (UniMAP)
No. 112 & 114, Tingkat 1, Blok A, Taman Pertiwi Indah,
Jalan Kangar-Alor Setar,
Seriab, 01000 Kangar, Perlis.

ACKNOWLEDGEMENTS

First and foremost, all praise, thanks and gratitude to Allah (SWT) who gave me the faith, strength, and insistence to complete this project. All purely thanks go to anyone who has contributed to the success of this work. Particularly, I would like to express my sincere gratitude and appreciation to my supervisor, **Dr. Ping Jack Soh,** who is understanding and easily adapted to the work when I met him after my previous supervisor left his job at the university. His continuous guidance, encouraging, valuable discussion and comments enhanced the work intensively and strengthed the scientific research values. I would also like to express my thanks and gratitude to **Prof. Dr. R. Badlishah Ahmad**, my co-supervisor, his suggestions and support during the period of study are valuable, and it helped me a lot particularly in the difficult time. All thanks to the UniMAP staff, especially the School of Computer and Communication staff.

I thank my previous main supervisors, **Dr. Fareq Malek**, he was so kind during the time when I was working with him, and Dr**. Abid Yahya**, who was a short-lived star in the period of my study. I wish them well in their new position and future career.

My special thanks go to **Prof. Dr. Bassim H. Hameed,** for his precious advice and all my friends during my academic period.

Last, but not least, the sincerest gratitude to my family specifically, to my mother, special thanks to my wife and kids to support me in the hard circumstances. Also to my brothers and sisters, their daily prayers gave me the motivation and strength towards my goals, and also to everyone who supported and prayed for me.

Mohammed Taih Gatte
School of Computer and Communication Engineering
University Malaysia Perlis (UniMAP)

TABLE OF CONTENTS

	PAGE
DECLARATION OF THESIS	**I**
PERMISSION TO USE	**II**
ACKNOWLEDGEMENTS	**III**
TABLE OF CONTENTS	**IV**
LIST OF TABLES	**VIII**
LIST OF FIGURES	**XI**
LIST OF ABBREVIATIONS	**XVII**
LIST OF SYMBOLS	**XX**
ABSTRAK	**XXII**
ABSTRACT	**XXIII**
CHAPTER 1: INTRODUCTION	1
1.1 Background	1
1.1.1 The MMW and THz Spectrum	2
1.1.2 Antennas Challenges in MMW and THz	3
1.1.3 Carbon Allotropes Nanomaterials	5
1.1.4 Graphene Specific Properties and Promising Application	6
1.2 Research Motivations	7
1.3 Problem Statement	8
1.4 Objectives	9
1.5 The Contribution of Thesis	10
1.6 Scope of Study	11
1.7 Thesis Organization	12

CHAPTER 2: LITERATURE REVIEW 14

2.1 Introduction 14

2.2 Overview of Microstrip Antennas 15

2.2.1 Microstrip Antennas 16

2.2.2 Features of Microstrip Antenna 18

2.2.3 Microstrip Antenna Feeding Techniques 19

2.2.4 Microstrip Antenna Figure of Merits 20

2.3 Overview of Millimeter Wave and THz Antennas 22

2.3.1 Millimeter Wave Antennas 22

2.3.2 THz Antennas 24

2.4 The Materials of Antenna 25

2.4.1 Conducting Materials 25

2.4.2 Dielectric Materials 28

2.4.3 New Materials for Antennas 29

2.5 Carbon Nanomaterials Overview 30

2.5.1 Graphene in Antenna Applications 31

2.5.2 Graphene Surface Properties 36

2.5.3 The Main Effected Parameters on Graphene Properties 38

2.5.4 Production of Graphene 38

2.5.5 Modeling of Graphene Depositing on Antenna Substrate 40

2.5.6 The Effect of Coating Metal Conductor via Graphene 41

2.5.7 Adhesive of Graphene Coated Metal to The Dielectric Substrate 42

2.6 Summary 44

CHAPTER 3: METHODOLOGY 46

3.1 Introduction 46

3.2 Materials and Methods for MMW and THz Microstrip Antenna Design 47
3.2.1 Geometric Modeling of Microstrip Antennas 48
3.2.2 Microstrip Antennas with Different Patch Shapes 51
3.2.3 Substrate Materials of Microstrip Antennas 52
3.2.4 Conducting Materials of Microstrip Antennas 53
3.2.5 Surface Properties of Graphene 54
3.2.6 Modeling of Graphene Based on Surface Properties 56
3.2.7 Characterization of Graphene Model Based on Surface Properties 57
3.3 Deposition of Graphene on Antenna Substrate 58
3.3.1 Configuration 1 with Different Graphene Models 59
3.3.2 Configuration 2 with Different Doped Graphene as Ground 60
3.3.3 Configuration 3 Different Graphene Doping for Both Conducting Layers 61
3.4 The Effect of Patch Topologies on THz Antenna 62
3.4.1 Behavior of the Doped Graphene-Based Patch Antennas 64
3.5 Coating Antenna Conducting Layers with Graphene 64
3.5.1 Graphene Deposition on the Conducting Layers of Antenna 65
3.6 Adhesion of Graphene Layer on the Antenna Substrate 67
3.7 Frequency Optimization for Graphene-based Antenna Utilization 70
3.7.1 Conductor Losses of Graphene and Copper Based Antennas 73
3.8 The Effect of Graphene on Antenna Figures-of-Merit 74
3.9 Summary 74

CHAPTER 4: RESULTS AND DISCUSIONS 76
4.1 Introduction 76
4.2 Modeling and characterization of monolayer graphene 77
4.2.1 Surface properties characterization based on chemical potential 77

4.2.2 Graphene surface properties characterization according to temperature 79

4.2.3 Graphene surface properties characterization based on relaxation time 81

4.3 Modeling of the graphene based antenna conducting layers 82

4.3.1 Graphene models as the antenna conducting layers 82

4.3.2 The effect of doped graphene on THz antenna behavior 84

4.3.3 The effect of doped graphene on MMW antenna behavior 89

4.4 Modeling of fabrication techniques for graphene based antenna 93

4.4.1 The Effect of Conducting Layers Coating by Graphene 95

4.4.1.1 The graphene coating effect on power radiated and power loss 98

4.4.1.2 The effect of coating by graphene on S11 and bandwidth 102

4.5 The critical frequency for none doped graphene 102

4.5.1 The CrFr According to Gain and Radiation Efficiency 107

4.5.2 CrFr According to Radiated Power and Metal Loss 117

4.5.3 The CrFr's of Antennas According to Models and Parameters 127

4.6 The Effect of Using Graphene on The Antenna Figures-of-merit 128

4.7 Summary 131

CHAPTER 5: CONCLUSIONS AND FUTURE WORKS 133

5.1 Conclusions 133

5.2 Future Works 136

REFERENCES 138

LIST OF PUBLICATIONS 149

LIST OF TABLES

NO		PAGE
2.1	The resistivity and conductivity of some common conducting materials	26
2.2	Table of metals activity for oxidization and corrosion	27
2.3	Performance Comparison of the proposed antennas compared to previous graphene based antenna investigations reported in literature	36
3.1	Parameters for the proposed patch antenna	50
3.2	Parameters for the proposed patch antenna	62
3.3	Rectangular(and elliptical) Patch Geometric Design Parameters	70
3.4	Hexagonal Patch Geometric Design Parameters	71
3.5	The computed parameters for each configuration of each topology	73
4.1	Performance comparison of microstrip patch antennas when various materials are used as both conducting layers	83
4.2	Performance comparison of the proposed rectangular and elliptical patch using copper (pure), non-doped and doped graphene	85
4.3	Performance comparison of the proposed antennas compared to previous graphene based antenna reported in literature	89
4.4	The effect of D-G on MMW antenna behavior	90
4.5	The antenna performance when different graphene fabrication techniques are employed at MMW and THz frequency bands for ND-G	94
4.6	The antenna performance when different graphene fabrication techniques are employed at MMW and THz frequency bands for a (0.5eV μc) D-G	94
4.7	Performance comparison of the patch antennas for the three above configurations Cn, Cp and Cb	96

4.8	The parameters for a rectangular microstrip antenna based on graphene	103
4.9	The parameters for a rectangular microstrip antenna based on copper	103
4.10	The parameters for a rectangular antenna with a graphene based patch	103
4.11	The parameters for rectangular antenna with a graphene based ground	104
4.12	The parameters for an elliptical microstrip antenna based on graphene	104
4.13	The parameters for an elliptical microstrip antenna based on copper	104
4.14	The parameters for an elliptical antenna with graphene based patch	105
4.15	The parameters for an elliptical antenna with graphene based ground	105
4.16	The parameters for a hexagonal microstrip antenna based on graphene	105
4.17	The parameters for a hexagonal microstrip antenna based on copper	105
4.18	The parameters for a hexagonal antenna with graphene based patch	106
4.19	The parameters for a hexagonal antenna with graphene based ground	106
4.20	Gain and radiation efficiency of the rectangular antenna with C1 and C4 as its conducting layer	107
4.21	Gain and radiation efficiency of a rectangular antenna with C2 and C3 as its conducting layer	109
4.22	Gain and radiation efficiency of the elliptical antenna with C1 and C4 as its conducting layers	111
4.23	Gain and radiation efficiency of the elliptical antenna with C2 and C3 as its conducting layers	112
4.24	Gain and radiation efficiency of a hexagonal antenna with C1 and C4 as its conducting layers.	114
4.25	Gain and radiation efficiency of a hexagonal antenna with with C2 and C3 as its conducting layers	115

4.26 Radiated power and metal loss of a rectangular antenna with C1 and C4 as its conducting layers 117

4.27 Radiated power and metal loss of a rectangular antenna with C2 and C3 as its conducting layers 119

4.28 Radiated power and metal loss of an elliptical patch with C1 and C4 as its conducting layers 121

4.29 Radiated power and metal loss of an elliptical antenna with C2 and C3 as its conducting layers 123

4.30 Radiated power and metal loss of a hexagonal antenna with C1 and C4 as its conducting layers 124

4.31 Radiated power and metal loss for a hexagonal antenna with C2 and C3 as its conducting layers 126

4.32 The effect of patch topology and antenna performance parameter on the critical frequency for C1 and C4 conducting layer models 128

4.33 The effect of patch topology and antenna performance parameter on the critical frequency for C2 and C3 conducting layer models 128

4.34 Rectangular antenna FoM: Q-factor, bandwidth, and radiation efficiencies for configurations C1 and C4 129

4.35 Hexagonal antenna FoM: Q-factor, bandwidth, and radiation efficiencies for configurations C1 and C4 129

4.36 Elliptical antenna FoM: Q-factor, bandwidth, and radiation efficiencies for configurations C1 and C4 130

LIST OF FIGURES

NO		PAGE
1.1	Architecture of a typical wireless sensor node and the significance of efficient antenna in such applications.	1
1.2	The bands of electromagnetic spectrum and their applications (Galoda & Singh, 2007)	3
1.3	Nano sensors wireless networks in health monitoring (Akyildiz et al., 2014)	5
1.4	The graphene layer structure (Russer et al., 2010)	5
1.5	Dissertation Overview	12
2.1	Geometry of rectangular patch antenna (Balanis, 2005)	17
2.2	Samples of microstrip antenna feeding techniques (a) inset gap (b) quarter wave length	19
2.3	The sample reflected radiation with negligible surface roughness of indicating that,(a) the metal oxide structure, and internal reflection (b) TL model, Z_I is the input surface impedance (Headland et al., 2016)	28
2.4	Nano patch based on GNR and Nano dipole based on CNT (Jornet & Akyildiz, 2010)	31
2.5	(a) Flexible conducting material based on graphene (b) Prototype of fabricated patch antenna based on graphene (Sajal et al., 2015)	33
2.6	Transmission measurement between two printed graphene wearable antennas (X. Huang et al., 2015)	34
2.7	Monolayer graphene deposited on Copper foil (Graphenea.com, 2015)	39
2.8	Monolayer graphene deposited on SiO2/Si (Graphenea.com, 2015)	39

2.9	The steps for the transfer method of graphene (Gupta et al., 2014)	43
3.1	The flow diagram for graphene based microstrip antenna design in the MMW and THz bands	47
3.2	The model of the rectangular microstrip patch antenna with an inset feed	51
3.3	Conductivity of Graphene	56
3.4	Surface Impedance of Graphene (modeling of graphene)	56
3.5	Flow chart of the modeling of graphene based antenna according to the direct deposition technique	59
3.6	Configuration 1 of the rectangular microstrip patch antenna when (a) ND-G and (b) D-G are used as patch layer	60
3.7	Configuration 2 of the rectangular microstrip patch antenna when (a) ND-G and (b) D-G are used as ground plane based on direct deposition technique	61
3.8	Microstrip ectangular patch antenna (a) CBA and (b) GBA according to direct deposition technique	61
3.9	The antenna geometrical topologies (a) and (b) front side with the ground plane (c) on the reverse side and (d) cross section of the elliptical patch	63
3.10	Flow diagram of the GBA design using the coating technique	65
3.11	Coating or deposition of ND-G on (a) the radiator and (b) the ground of the rectangular patch antenna (Configuration 1&2)	66
3.12	(a) Coating or deposition of the ND-G on both conducting layers (patch and ground) of rectangular patch (Configuration 3) (b) Non-coated CBA	66
3.13	Flow diagram of the GBA design using the adhesive technique	67
3.14	Adhesion of the CVD-graphene film (graphene coated copper) on antenna substrate (a) for patch (Configuration 1) (b) for ground (Configuration 2)	69

3.15 (a) Adhesion of the CVD-graphene film (graphene coated copper) on antenna substrate as patch and ground (Configuration 3) (b) CBA 69
3.16 Hexagonal 64 GHz microstrip patch antenna 71
3.17 Flow diagram for the calculation the critical frequencies of ND-G the use of GBA in the MMW and THz bands 72
4.1 The complex surface conductivity of graphene characterized based on different values of chemical potentials 78
4.2 Calculated surface impedance of graphene in the MMW band for different chemical potentials 79
4.3 Calculated surface impedance of graphene in the THz and infrared bands for different chemical potentials 79
4.4 Calculated surface impedance of graphene in the MMW and THz bands at 0eV chemical potential and different temperatures 80
4.5 Calculated surface impedance of graphene in the THz and infrared bands at 0eV chemical potential and different temperatures 80
4.6 Calculated surface impedance of graphene in the MMW and THz bands at 0eV chemical potential, 300k temperature and different relaxation times 81
4.7 Calculated surface impedance of graphene in the THz and infrared bands at 0eV chemical potential, 300K temperature and different relaxation times 82
4.8 Radiated power: for different patches based on copper and different models of graphene 87
4.9 Reflection coefficients for different patches based on copper and different models of graphene 87
4.10 The far field radiation pattern of the D-G for different patches: Elliptical shows better performance than rectangular patch at both frequencies 88

4.11 Antenna reflection coefficients using different conductive materials 91
4.12 Accepted power of the antenna using different conductive materials 91
4.13 Radiated power of the antenna using different conductive materials 92
4.14 Dielectric loss of the antenna when using different conductive materials 92
4.15 Metal loss of the antenna when using different conductive materials 93
4.16 Far field radiation pattern for the non-coated antenna (Cn) 96
4.17 Far field radiation pattern for the graphene-coated patch only (Cp) 97
4.18 Far field radiation for the graphene-coated both patch and ground (Cb) 97
4.19 Power loss for the non-coated antenna (Cn) 98
4.20 Power loss for the graphene-coated patch (Cp) antenna 99
4.21 Power loss for the graphene-coated patch and ground (Cb) antenna 99
4.22 The power loss comparison for non-coated (Cn), patch-coated (Cp), patch and ground-coated (Cb) antennas 100
4.23 The dielectric loss comparison for non-coated (Cn), patch-coated (Cp), patch and ground-coated (Cb) antennas 101
4.24 The radiated power comparison for non-coated (Cn), patch-coated (Cp), patch and ground-coated (Cb) antennas 101
4.25 The reflection coefficient (S11) comparison for non-coated (Cn), patch-coated (Cp) and patch and ground-coated (Cb) antennas 102
4.26 The gain curves of the ND-G based rectangular antenna models along FBOI. Inset shows its CrFr at 0.16 THz 108
4.27 The radiation efficiency curves of the ND-G based rectangular antenna models along FBOI. Inset shows its CrFr at 0.171 THz 108
4.28 The gain curves of the ND-G based rectangular antenna models along FBOI. Inset shows its CrFr at 0.19 THz 110

4.29 The radiation efficiency curves of the ND-G based rectangular antenna models along FBOI. Inset shows its CrFr at 0.24 THz 110
4.30 The gain curves of the ND-G based elliptical antenna models along FBOI. Inset shows its CrFr at 0.15 THz 111
4.31 The radiation efficiency curves of the ND-G based elliptical antenna models along FBOI. Inset shows its CrFr at 0.145 THz 112
4.32 The gain curves of the ND-G based elliptical antenna models along FBOI. Inset shows its CrFr at 0.154 THz 113
4.33 The radiation efficiency curves of the ND-G based elliptical antenna models along FBOI. Inset shows its CrFr at 0.145 THz 113
4.34 The gain curves of the ND-G based hexagonal antenna models along FBOI. Inset shows its CrFr at 0.127 THz 114
4.35 The radiation efficiency curves of the ND-G based hexagonal antenna models along FBOI. Inset shows its CrFr at 0.13 THz 115
4.36 The gain curves of the ND-G based hexagonal antenna models along FBOI. Inset shows its CrFr at 0.2 THz 116
4.37 The radiation efficiency curves of the ND-G based hexagonal antenna models along FBOI. Inset shows its CrFr at 0.18 THz 116
4.38 The radiated power curves of the ND-G based rectangular antenna models along FBOI. Inset shows its CrFr at 0.224 THz 118
4.39 The metal loss curves of the ND-G based rectangular antenna models along FBOI. Inset shows its CrFr at 0.162 THz 118
4.40 The radiated power curves of the ND-G based rectangular antenna models along FBOI. Inset shows its CrFr at 0.28 THz 120

4.41 The metal loss curves of the ND-G based rectangular antenna models along FBOI. Inset shows its CrFr at 0.365 THz 120

4.42 The radiated power curves of the ND-G based elliptical antenna models along FBOI. Inset shows its CrFr at 0.131 THz 122

4.43 The metal loss curves of the ND-G based elliptical antenna models along FBOI. Inset shows its CrFr at 0.152 THz 122

4.44 The radiated power curves of the ND-G based elliptical antenna models along FBOI. Inset shows its CrFr at 0.177 THz 123

4.45 The metal loss curve of the ND-G based elliptical antenna models along FBOI. Inset shows its CrFr at 0.185 THz 124

4.46 The radiated power curves of the ND-G based hexagonal antenna models along FBOI. Inset shows its CrFr at 0.24 THz 125

4.47 The metal loss curves of the ND-G based hexagonal antenna models along FBOI. Inset shows its CrFr at 0.15 THz 125

4.48 The radiated power curves of the ND-G based hexagonal antenna models along FBOI. Inset shows its CrFr at 0.31 THz 126

4.49 The metal loss curves of the ND-G based hexagonal antenna models along FBOI. Inset shows its CrFr at 0.14 THz 127

LIST OF ABBREVIATIONS

AB	Adhesive bonding
AWB	Adhesive wafer bonding
CBA	Copper Base Antenna
CNTs	Carbon Nanotubes
CrFr	Critical Frequency
CST (MWS)	Computer Simulation Technology (Microwave Studio)
Cu	Copper
CVD	Chemical Vapor Deposition
1D	One Dimension
2D	Two Dimensions
3D	Three Dimensions
DC	Direct Current
D-G	Doped Graphene
DGS	Defected Ground Structure
EBG	Electromagnetic Band Gap
EMETS	Electromagnetic Engineering Tools Solver
EM	Electromagnetic
FBOI	Frequency Band of Interest
FCC	Federal Communications Commission
GBA	Graphene Base Antenna
GHz	Gigahertz
GNR	Graphene Nano-Ribbon

HDRC	High Data Rate Communication
HQMG	High-Quality Monolayer Graphene
HQG	high-quality graphene
IR	Infrared
LCP	Liquid crystal polymer
MEMs	microelectromechanical systems
MLG	Mono Layer Graphene
MMW	Millimeter Wave
MST	Modulated Scattering Technique
MW	Microwave
MWNT	Multi-Walled Carbon Nanotubes
ND-G	Non-Doped Graphene
Ni	Nickle
PC/ABS	Polycarbonate/acrylonitrile butadiene styrene
PCB	Printed Circuit Board
PDMS	Polydimethylsiloxane
PEC	Perfect Electrical Conductor
PET	Polyethylene terephthalate
PMMA	Poly(methyl methacrylate)
PTP	Point-to-Point
PTMP	Point-to-Multi Point
RF	Radio frequency
RFID	Radio-Frequency Identification
RLO	Regulations for Licensed Operation
RSW	Reduced Surface Wave

RULO	Regulations for Unlicensed Operation
SMA	Simple Matching Approach
SWNTs	Single-Walled Carbon Nanotubes
THz	Terahertz
TL	Transmission line
ULB	Unlicensed Band
WiMAX	Worldwide Interoperability for Microwave Access
WSN	Wireless sensors networks

LIST OF SYMBOLS

C	Speed of Light
fr	Frequency Resonance
λ	Resonance Wavelength
λ_{eff}	Effective Resonance Wavelength
ϵ_r	Dielectric Constant
ϵ_{reff}	Effective Dielectric Constant
μ	Relative Permeability
h	Thickness of Substrate
W	Patch Width
W_n	Iteration Patch Width
Wp	Patch Width
L	Patch Length
Lp	Patch Length
ΔL	Extended in Patch Length
Wf	Feed Line Width
Lf	Feed Line Length
Wg	Feed Gap Width
Lg	Feed Gap Length
D	Directivity
Dir	Directivity
G	Gain
η	Radiation Efficiency

ηr	Radiation Efficiency
P_{rad}	Radiated Power
L_{met}	Metal Loss
S11	the absolute value of return loss
Γ	Return Loss
VSWR	Voltage Standing Wave Ratio
Q_c	conduction (ohmic) losses quality factor
Q_d	dielectric losses quality factor
Q_{rad}	radiation (space wave) losses quality factor
Q_{sw}	surface waves loss quality factor
Q_t	Total quality factor
ρ	Resistivity
δ	The substrate material loss tangent
σ	Conductivity
σ_s	Surface Conductivity
Z_s	Surface Impedance
μc	Chemical Potential
q_e	Electron charge
τ	Relaxation Time
δ_s	skin depth
T	Temperature
j	Imaginary Unit
K_B	Boltzman's Constant
$\hbar$	Reduce Blanck Constant

Pemodelan dan Pencirian Graphene untuk Antena Gelombang Milimeter dan TeraHertz Berkecekapan Tinggi

ABSTRAK

Pembangunan teknologi gelombang millimeter (MMW) dan Terahertz (THz) untuk sistem penderiaan tanpa wayar dan aplikasi komunikasi telah berlaku dengan pesat disebabkan ciri-ciri unik gelombang dalam jalur-jalur ini. Antena merupakan salah satu elemen teras dalam aplikasi komunikasi, manakala pembangunan antena berkecekapan tinggi dalam jalur-jalur gelombang ini memerlukan penggunaan bahan nanokarbon seperti graphene. Ini adalah disebabkan oleh kemerosotan konduktivi logam konvensional dengan peningkatan frekuensi. Penyelidikan ini berfokus untuk menambahbaik prestasi antena dalam jalur MMW dan THz dengan menggunakan graphene. Penggunaan graphene memerlukan pemodelan matematik dan pencirian sifat permukaannya yang berubah mengikut frekuensi. Perubahan beza upaya kimia (μc) (menerusi pendopan) menunjukkan kesan yang lebih ketara berbanding parameter yang lain. Perubahan ini adalah bergantung kepada pincangan elektrik, pincangan magnetik atau pendopan kimia. Nilai μc = 0eV digunakan dalam model graphene yang tidak terdop (ND-G), manakala nilai-nilai μc = 0.25eV and μc = 0.5eV diguna dalam model graphene yang didop (D-G). D-G didapati menunjukkan nilai konduktiviti permukaan yang lebih tinggi berbanding ND-G, manakala peningkatan μc menyebabkan peningkatan konduktiviti graphene. Model graphene (D-G dan ND-G) kemudiannya diintegrasikan ke atas substrat dan dimasukkan ke dalam perisian penyelesai mikro gelombang CST sebelum disimulasikan untuk menentukan prestasi antena berasaskan graphene (GBA) ini. Model-model GBA ini turut menunjukkan penambahbaikan prestasi yang signifikan berbanding model-model berasaskan tembaga(1 THz, 1.29 THz, dan 1.49 THz). Walaubagaimanapun, penggunaan ND-G tidak selalunya menunjukkan peningkatan prestasi yang ketara pada frekuensi MMW (64GH), tetapi peningkatan prestasi ini lebih tertumpu kepada jalur operasi yang lebih tinggi. Dua teknik lain (salutan dan lekatan) dicadang sebagai kaedah fabrikasi alternatif bagi antena-antena berasaskan graphene. Teknik-teknik ini menunjukkan penambahbaikan prestasi yang sama berbanding dengan teknik pemendapan terus dalam jalur-jalur MMW (70GHz) dan THz (1.71 THz). Kajian ini turut menunjukkan bahawa model antena menggunakan teknik lekatan menunjukkan prestasi yang lebih baik berbanding teknik pemendapan terus pada frekuensi MMW. Seterusnya, suatu kajian untuk menentukan frekuensi kritikal (CrFr) bagi penggunaan ND-G dan tembaga pada frekuensi MMW dan THz telah dijalankan (30GHz-3THz). Kajian ini mempertimbangkan topologi dan parameter prestasi ND-G-GBA untuk menentukan CrFr. Keluk-keluk parameter prestasi diplotkan melawan frekuensi untuk memudahkan perbandingan di antara pelbagai konfigurasi GBA. CrFr ditunjukkan pada titik-titik persilangan di antara keluk-keluk parameter prestasi bagi antena berasaskan tembaga dan antena berasaskan graphene. Kajian ini turut dilanjutkan untuk GBA di mana graphene digunakan sama ada sebagai bumi atau pemancar sahaja. Perbandingan topologi, konfigurasi dan parameter antena yang berbeza menunjukkan CrFr yang berbeza, di antara 0.130 – 0.240 THz, dengan purata 0.147 THz. Manakala bagi konfigurasi antena yang menggunakan graphene sahaja sebagai bumi atau pemancar, frekuensi kritikal didapati berada di antara 0.145 – 0.365 THz, dengan purata 0.213 THz. Ini menunjukkan bahawa CrFr untuk ND-GBA adalah bergantung kepada topologi antena serta konfigurasinya.

Modeling and Characterization of Graphene for Efficient Millimeterwave and THz Antennas

ABSTRACT

The development of millimeterwave (MMW) and Terahertz (THz) technologies for a wide range of wireless sensing and communication applications have been rapid due to the unique characteristics of waves in these bands. Antennas are regarded as the core of wireless applications, and its development for efficient operation within these bands require the use of new carbon nanomaterials such as graphene. This is due to the conductivity deterioration of conventional metals with increasing frequency. This work focuses on improving the antenna performance parameters in the MMW and THz bands based on the utilization of graphene. The employment of graphene requires mathematical modelling and characterization of its surface impedance, which are frequency dependent. The chemical potential (μc) (doping) indicated a more significant effect compared to other variables. Its values are influenced by electrical bias, magnetic bias, or chemical doping. The μc = 0eV value is used as the non-doped graphene (ND-G) model, while (μc = 0.25eV and μc = 0.5eV) values are used for the doped graphene (D-G) models. D-Gs were found to exhibit higher surface conductivities than ND-G, while the increasing μc resulted in increased graphene conductivity. The material models of graphene (D-G and ND-G) are then integrated onto the substrate and the microwave solver software CST prior to simulations to determine the graphene based antenna (GBA) performance. These GBA antenna models indicated significant performance improvement at THz frequencies (1 THz, 1.29 THz, and 1.49 THz) compared to the copper-based antenna models. On the contrary, the use of ND-G does not always show such significant improvements at MMW frequencies (64GH), but is rather more concentrated on the bands beyond it. Two other new techniques (coating and adhesives) are proposed as alternative fabrication methods of graphene based antennas. These techniques indicated similar parameter improvements to that of the direct deposition technique in the MMW (70GHz) and THz (1.71 THz) bands. It was also discovered that antenna modeling using the adhesive technique performs better than the direct deposition technique at MMW frequencies. Next, an investigation to determine the critical frequency (CrFr) for the use of ND-G and copper at MMW and THz spectrum (30GHz-3THz) was performed. This study considers different topologies and performance parameters of ND-GBA to determine CrFr. The curves of the performance parameters are plotted against frequency to facilitate comparison between various GBA configurations. The CrFr is determined using the intersections of the performance curves for copper-based and graphene-based antenna. The investigation is also extended onto GBAs with graphene as ground or patch only. The comparison for different antenna topologies, configurations, and parameters reported different CrFrs, ranging from 0.130 - 0.240 THz, with an average of 0.147 THz. On the other hand, the critical frequencies for the patch and ground only graphene-based configurations ranged between 0.145 - 0.365 THz, with an average of 0.213 THz indicating that the CrFr of ND-GBA depends on the antenna topologies and configurations.

CHAPTER 1

INTRODUCTION

1.1 Background

Antennas are cohesively related to wireless communications and wireless sensing networks (WSN). Beside wireless communications, antennas are also crucial towards other applications such as imaging, spectroscopy, sensing, detection, and energy harvesting, particularly in frequency spectrums higher than microwaves (MW) band such as millimeter wave (MMW) terahertz (THz) and infrared (IR). Figure 1.1 shows the architecture of typical wireless sensor nodes and the significance of efficient antenna to more than one unit in the node.

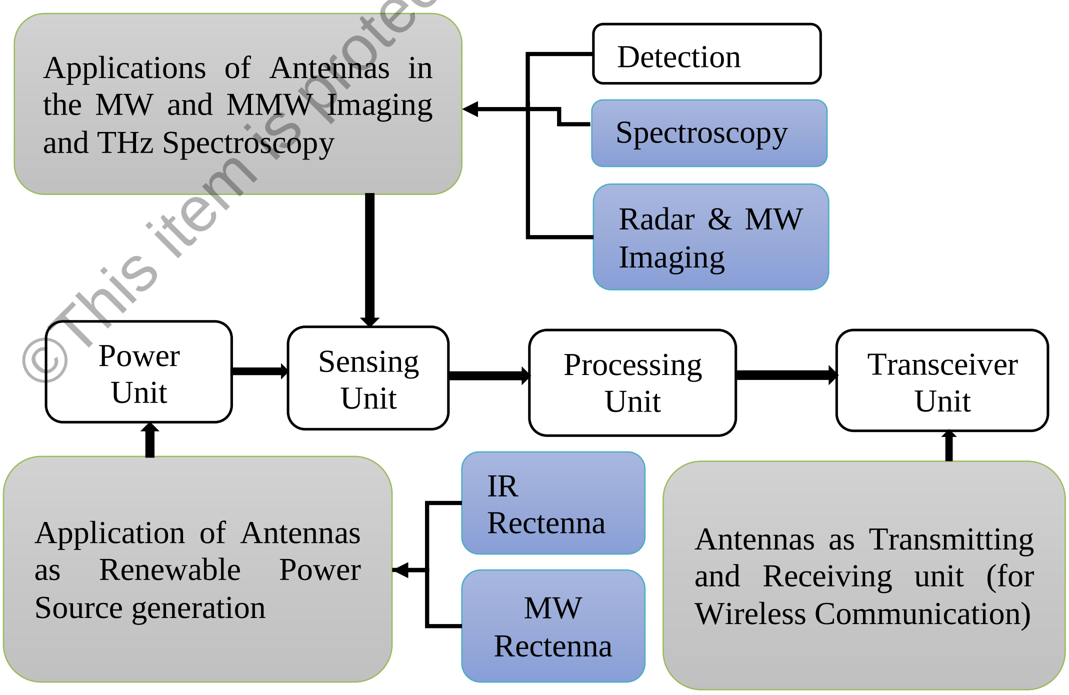

Figure 1.1: Architecture of a typical wireless sensor node and the significance of efficient antenna in such applications.